

Supplemental Methods

In situ hybridization procedures

Slide-mounted tissue sections were immersed in 4% paraformaldehyde in phosphate buffered saline (PBS), acetylated, dehydrated through a graded ethanol series, and de-fatted in chloroform for 10 min. The sections were then incubated with ³⁵S-labeled riboprobes in hybridization buffer containing 50% formamide, 0.75 M NaCl, 20 mM 1,4-piperazine diethane sulfonic acid, pH 6.8, 10 mM EDTA, 10% dextran sulfate, 5X Denhardt's solution, 50 mM dithiothreitol, 0.2% SDS and 100 mg/ml yeast tRNA at 56°C for 16 hrs. After washing in a solution containing 0.3 M NaCl, 20 mM Tris-HCl, pH 8.0, 1 mM EDTA, pH 8.0, and 50% formamide at 63°C, the sections were treated with RNase A (20 µg/ml) at 37°C, and washed in 0.1x SSC (150 mM NaCl and 15 mM sodium citrate) at 66.8°C. Sections were then dehydrated through a graded series of ethanol concentrations, air dried, and exposed to BioMax MR Film (Kodak, Rochester, NY). After exposure to film, sections were coated with NTB emulsion (Kodak; diluted 2:1 with water).

Analyses were performed by one investigator (JGMA) without knowledge of diagnosis or subject number due to random coding of the sections. Trans-illuminated autoradiographic film images were captured by a video camera under controlled conditions, digitized, and analyzed with a Microcomputer Imaging Device (MCID) system (Imaging Research Inc, London, Ontario, Canada). Images of the corresponding hybridized sections were captured and superimposed on the autoradiographic images to draw contours and delineate the border between gray matter and white matter. Optical density was measured within the contours and expressed as nanocuries per

gram of tissue, determined by reference to ^{14}C standards (ARC Inc., St. Louis, MO) exposed on the same film.

Studies in monkeys

For the antipsychotic-exposed monkey cohort, serial cryostat sections (16 μm) were cut from fresh frozen tissue blocks containing the middle one-third of the principal sulcus. Two sections from each animal, spaced at 224 μm , were used to analyze δ mRNA expression in DLPFC areas 9 and 46, identified according to cytoarchitectonic criteria in Nissl sections (1). Sections from each triad were processed together in a single *in situ* hybridization run; two runs were performed.

The animals in the developmental cohort were divided into seven age groups to study the postnatal development of δ and $\alpha 4$ mRNA expression in the DLPFC. In some animals (Supplemental Table 2), the brain was removed immediately after euthanasia, whereas other animals were perfused transcardially with ice-cold modified artificial cerebrospinal fluid (aCSF) at the time of euthanasia (2). In some of the latter animals, a small block of tissue was surgically excised from the rostral third of the principal sulcus in the left hemisphere 2-4 weeks prior to perfusion with aCSF for electrophysiology studies (2). In order to control for the possible effects of neurosteroids on the expression of δ -containing receptors (3), menstrual status was determined for the post-pubertal 42-month and adult animals by assessing serum levels of estradiol and progesterone obtained immediately prior to euthanasia in 8 of 9 animals. For the remaining adult animal, records of observed menstruation indicated that she had very stable cycles which predicted that she was in the luteal phase at the time of euthanasia (Supplemental Table 2).

Serial coronal sections (16 μm) were cut through the caudal third of the principal sulcus in the right hemisphere of each monkey. Monkeys were divided into two groups, each containing

the same number of animals of each age. Two adjacent sections from each animal, spaced at 224 μm , were used to analyze the mRNA expression levels of δ and $\alpha 4$ mRNAs in area 46, identified according to cytoarchitectonic criteria in Nissl sections (1). Sections from each group were processed together in a single *in situ* hybridization run; four runs were performed. In addition, a section from a control animal was included in each *in situ* hybridization run to normalize for any experimental variability between runs.

For both cohorts, *in situ* hybridization procedures were performed as described above, except that the sections were not de-fatted in chloroform. Analyses of film autoradiograms were performed as described above without knowledge of animal number or experimental group. All procedures in both cohorts were carried out in accordance with the NIH Guide for the Care and Use of Laboratory Animals and were approved by the University of Pittsburgh Institutional Animal Care and Use Committee.

For the antipsychotic-treated monkeys, a single-factor ANOVA model was used, with triad as the blocking factor and treatment group as the main effect. Differences across postnatal development in the expression levels of δ and $\alpha 4$ mRNAs were assessed by ANCOVA models, with age group as the main effect and both perfusion and prior biopsy as blocking factors. Duncan's post hoc test was used to assess the differences between age groups for significant ANCOVAs.

Studies in rodents

GABA_A receptor $\alpha 1$ subunit knockout mice. We utilized tissue from mice with a targeted deletion of the GABA_A $\alpha 1$ subunit (4). As previously shown, the exon encoding nucleotides 1307 to 1509 of the $\alpha 1$ subunit was flanked by loxP sites and the knockout $\alpha 1$ allele was generated after cre-mediated recombination. Two groups of mice, wild type and $\alpha 1$ knockout

(KO), were euthanized at 8 weeks of age (n = 8 per group). Brains were frozen immediately and stored at -80°C. Serial coronal sections (12 µm) were cut from +1.98 to +1.54 bregma (5). Three sections, spaced at 144 µm, were selected from each animal and processed for *in situ* hybridization, using riboprobes generated from a 598 bp cDNA fragment of the δ subunit corresponding to bases 235-832 of the mouse gene (GenBank NM_008070), and from a 537 bp cDNA fragment of the $\alpha 4$ subunit corresponding to bases 655-1191 of the mouse gene (GenBank NM_010251). For $\alpha 4$ analysis, one *in situ* hybridization run containing sections from all 16 animals was performed. For the δ subunit, two *in situ* hybridization runs, each containing sections from four wild type and four $\alpha 1$ KO mice, were performed. Quantification of mRNA levels was done in the medial frontal cortex (MFC), including the cingulate and prelimbic cortices (5). Western blot studies confirmed a >95% reduction in $\alpha 1$ protein levels in the $\alpha 1$ KO mice (data not shown).

NMDA Nr1 hypomorphic mice. We utilized tissue from mice genetically engineered to express low levels of the NMDA receptor Nr1 subunit (NR1 hypomorphic mice). These mice were generated using homologous recombination in embryonic stem (ES) cells, utilizing a targeting vector to insert a neomycin resistance gene into intron 20 of the Nr1 locus (6). ES cells carrying the targeted mutation were used to generate mice with an altered Nr1 allele (*Nr1^{neo}*). Three groups of mice, wild type (*Nr1^{+/+}*), heterozygous (*Nr1^{neo/+}*) and homozygous (*Nr1^{neo/neo}*), were euthanized at 8 weeks of age (n = 4 for each group). Brains were frozen immediately and stored at -80°C. Serial coronal sections (12 µm) containing the MFC were cut (from +1.98 to +1.54 bregma (5)). Three sections (spaced at 144 µm) were selected from each animal and processed for *in situ* hybridization for each transcript, NMDA Nr1 and δ , as described above. Templates for the synthesis of mouse NMDA Nr1 were obtained by PCR with specific primer sets; a 517 bp cDNA

fragment for NMDA Nr1 corresponding to bases 1902-2418 of the mouse gene (GRIN1, GenBank NM_008169) was amplified. Nucleotide sequencing revealed 100% homologies for the amplified fragment to the previously reported sequences. One *in situ* hybridization run containing sections from all 12 animals was performed for each transcript. Quantification of NMDA Nr1 and δ mRNA levels was done in the MFC as described above.

Adult mediodorsal thalamic nuclei lesioned (MDTNL) rats. Two injections of 0.10 - 0.12 μ l ibotenic acid (5 μ g/ μ L) were made into each hemisphere (anteroposterior: -2.3 mm; lateral: +0.6 mm; dorsoventral: -5.5 mm) of peripubertal Sprague–Dawley rats (n = 8) (7). In sham rats (n = 8), the needle was lowered into the hippocampus, but did not penetrate the thalamus, and no injections were made. After a 4-week survival period, the animals were sacrificed by decapitation. The proportion of MDTN lesioned was previously determined (7), using Nissl-stained coronal sections through the entire extent of MDTN and the Cavalieri estimator of volume (8). Brains were frozen immediately and stored at -80°C. Serial coronal sections (12 μ m) containing the MFC were cut (from +3.7 to +2.2 mm bregma (9)). For the δ subunit, four sections (spaced at 240 μ m) were selected from each animal and processed for *in situ* hybridization. The mouse δ riboprobe was utilized to analyze the mRNA levels of δ in rat brains, since the 598 bp mouse cDNA amplified had 94% homology with the rat δ subunit (GenBank NM_017289); in addition, the mRNA expression pattern of δ across the rat MFC was similar to that observed in mice. Two *in situ* hybridization runs, each containing sections from all 16 animals, were performed. Quantification of δ mRNA levels was done in the MFC as described above.

Neonatal ventral hippocampal lesioned (NVHL) rats. At postnatal days 6-7, male Sprague–Dawley pups were anesthetized by hypothermia, placed on a stereotaxic frame and administered bilateral injections of sham (n = 11) or 0.3 μ L of ibotenic acid (10 μ g/ μ L, n = 13) into the ventral hippocampus (anteroposterior: -3.0 mm; lateral: +3.5 mm; dorso-ventral: -5.0 mm), as previously described (10). At postnatal 60-65 days of age, rats were anesthetized, and brains were removed, frozen immediately and stored at -80°C. Serial coronal sections (12 μ m) containing the MFC were cut (from +3.7 to +2.2 mm bregma (9)). Three sections (spaced at 180 μ m) were selected from each animal and processed for *in situ* hybridization with the δ mouse riboprobe. One *in situ* hybridization run containing sections from all 24 animals was performed. Quantification of δ mRNA levels was done in the MFC as described above. Qualitative assessments of lesion size were made for all animals with Nissl-stained sections spanning the entire rostrocaudal extent of the lesion, as previously described (10).

Statistical analyses. The expression of δ mRNA in the MFC of α 1 KO mice was analyzed with an ANCOVA model using genotype as main effect, and *in situ* hybridization run as a covariate since two *in situ* hybridization runs were performed. The mRNA levels of the α 4 subunit were analyzed with a two-sample t-test because only one *in situ* hybridization run was performed. To assess mRNA expression levels in the Nr1 hypomorphic mice, we performed an ANOVA model, using genotype as the main effect. Duncan's post hoc test was used to assess the differences between genotypes for significant ANOVAs. We used two-sample *t*-tests to examine the expression levels of δ subunit mRNA between sham and MDTNL animals, and between sham and NVHL animals. All statistical tests were conducted with an α -level = 0.05.

References

1. Barbas H, Pandya DN: Architecture and intrinsic connections of the prefrontal cortex in the rhesus monkey. *J Comp Neurol* 1989; 286:353-375
2. Gonzalez-Burgos G, Kroener S, Zaitsev AV, Povysheva NV, Krimer LS, Barrionuevo G, Lewis DA: Functional maturation of excitatory synapses in layer 3 pyramidal neurons during postnatal development of the primate prefrontal cortex. *Cereb Cortex* 2008; 18:626-637
3. Maguire JL, Stell BM, Rafizadeh M, Mody I: Ovarian cycle-linked changes in GABA(A) receptors mediating tonic inhibition alter seizure susceptibility and anxiety. *Nat Neurosci* 2005; 8:797-804
4. Vicini S, Ferguson C, Prybylowski K, Kralic J, Morrow AL, Homanics GE: GABA(A) receptor alpha1 subunit deletion prevents developmental changes of inhibitory synaptic currents in cerebellar neurons. *J Neurosci* 2001; 21:3009-3016
5. Paxinos, G. and Franklin, K. *The Mouse Brain in Stereotaxic Coordinates*. Second Edition. 2001. San Diego, Academic Press.
6. Mohn AR, Gainetdinov RR, Caron MG, Koller BH: Mice with reduced NMDA receptor expression display behaviors related to schizophrenia. *Cell* 1999; 98:427-436
7. Volk DW, Lewis DA: Effects of a mediodorsal thalamus lesion on prefrontal inhibitory circuitry: implications for schizophrenia. *Biol Psychiatry* 2003; 53:385-389

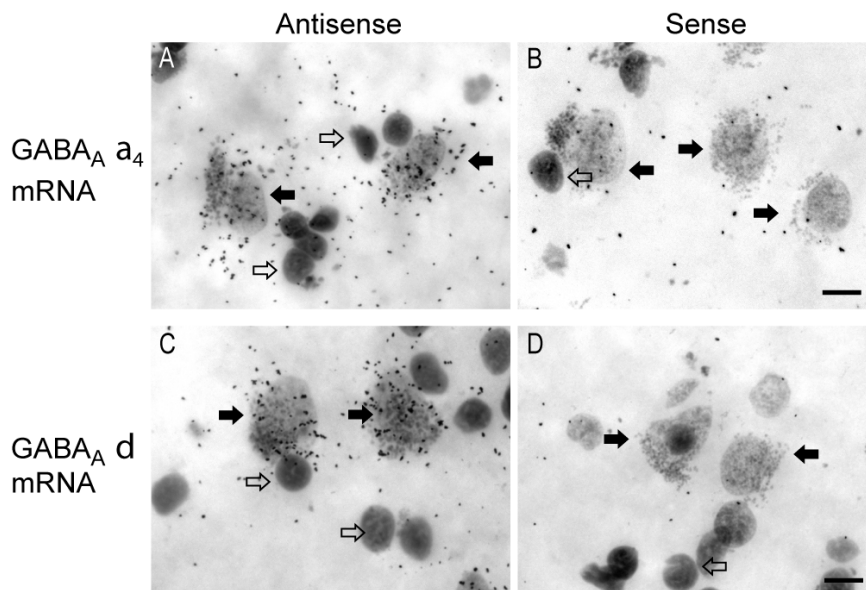
8. Howard CV, Reed MG: Unbiased stereology. Three-dimensional measurement in microscopy., vol. 0, 0 ed. Oxford, Bios Scientific Publishers, Ltd., 1998

9. Paxinos G, Watson C: The rat brain in stereotaxic coordinates, 2 ed. Orlando, Academic Press, 1986

10. O'Donnell P, Lewis BL, Weinberger DR, Lipska BK: Neonatal hippocampal damage alters electrophysiological properties of prefrontal cortical neurons in adult rats. *Cereb Cortex* 2002; 12:975-982

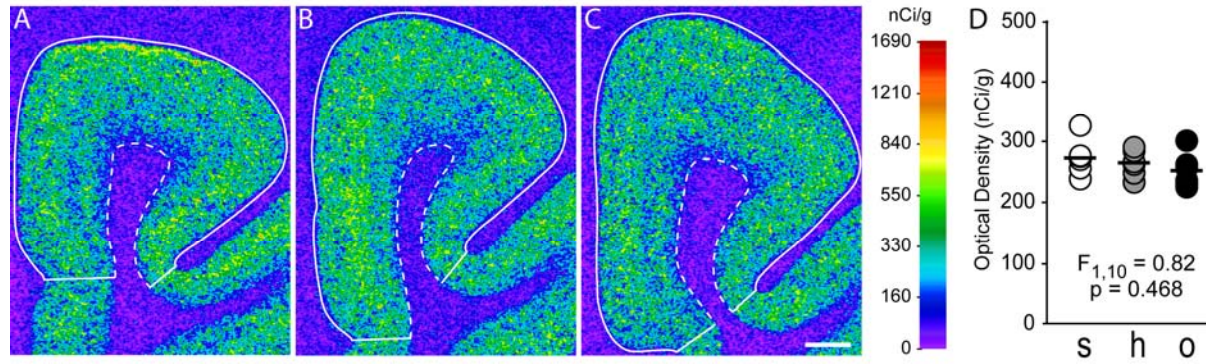
Supplemental Figures and Tables

Figure S1. Photomicrographs illustrating the expression of $\alpha 4$ and δ mRNAs in Nissl-stained, emulsion-dipped sections^a



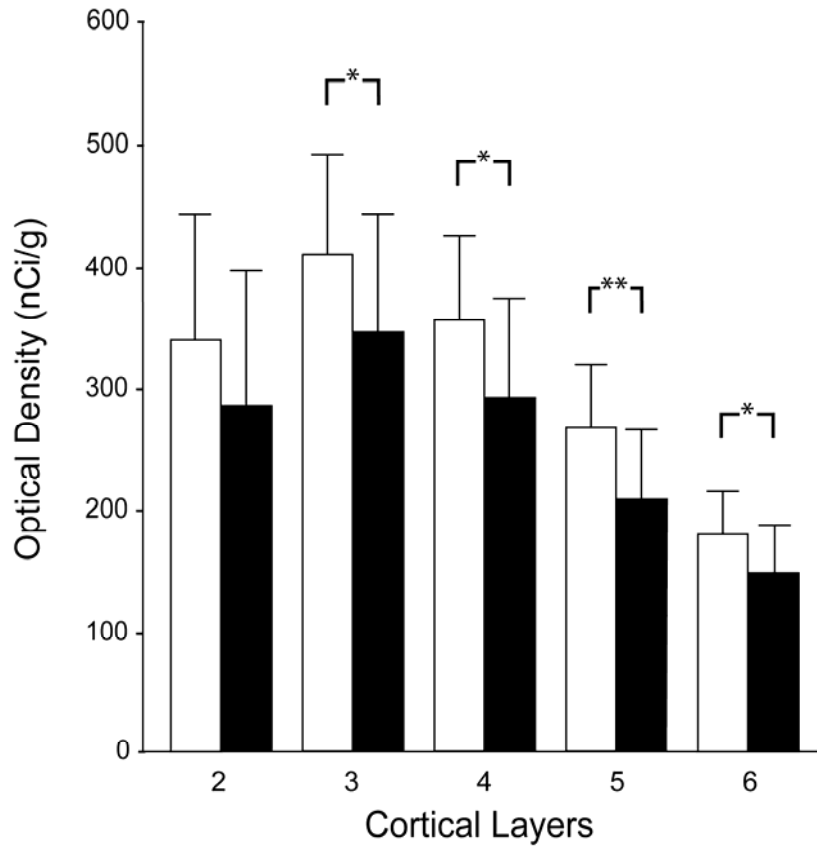
^a Sections processed with antisense riboprobes for $\alpha 4$ (A) and δ (C) mRNAs revealed specific clustering of silver grains over neurons (characterized by their faint Nissl-stain and large nuclei; solid arrows), but not over glia cells (characterized by their intensely Nissl-stained, small nuclei; open arrows). In addition, silver grain clustering over neurons was not observed in sections treated with $\alpha 4$ (B) or δ (D) sense riboprobes. Scale bars = 10 μ m.

Figure S2. Representative autoradiograms illustrating the expression of δ mRNA in the DLPFC of monkeys chronically exposed to sham (A), haloperidol (B) or olanzapine (C)^a



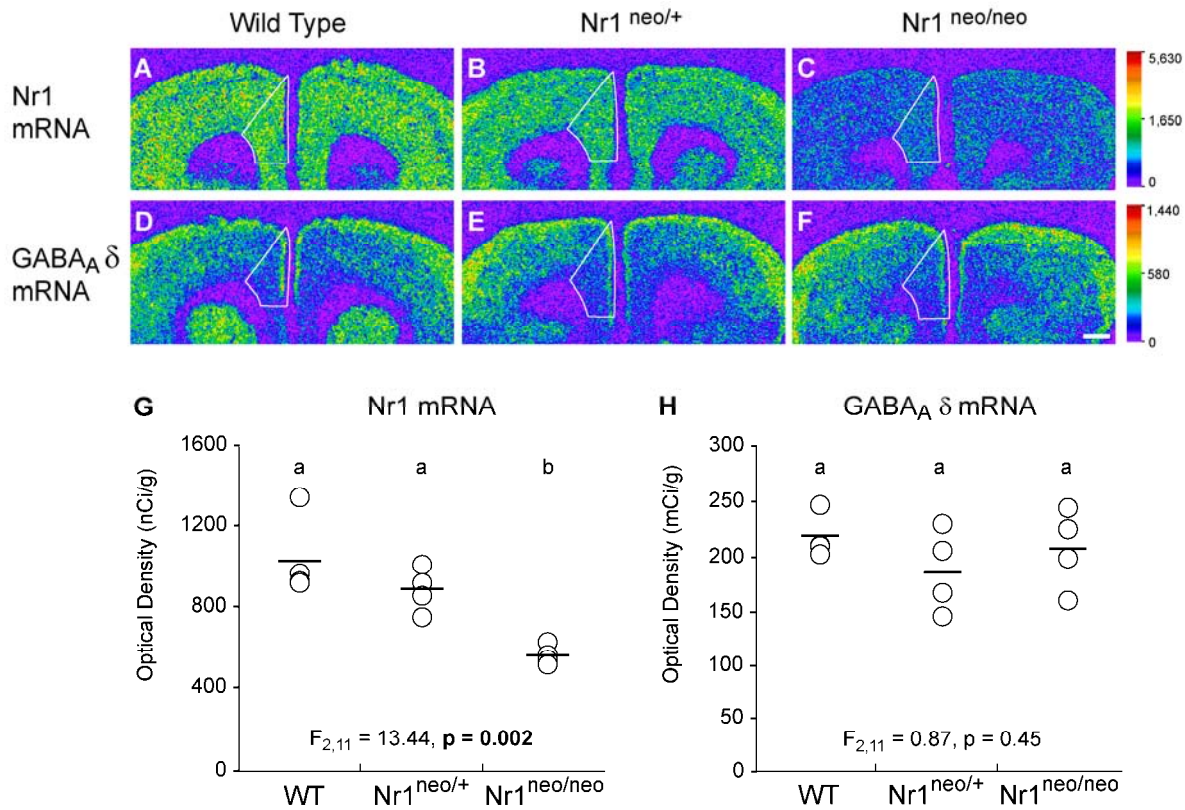
^a Solid lines represent the pial surface and the dotted lines represent the border between gray matter and white matter. The mean levels of δ mRNA did not differ across sham (s), haloperidol (h) or olanzapine (o) treated monkeys (D). The mean values for each subject group are represented by horizontal bars. Scale bar = 1 mm.

Figure S3. Mean film autoradiogram optical density measures for δ mRNA across cortical layers of the DLPFC^a



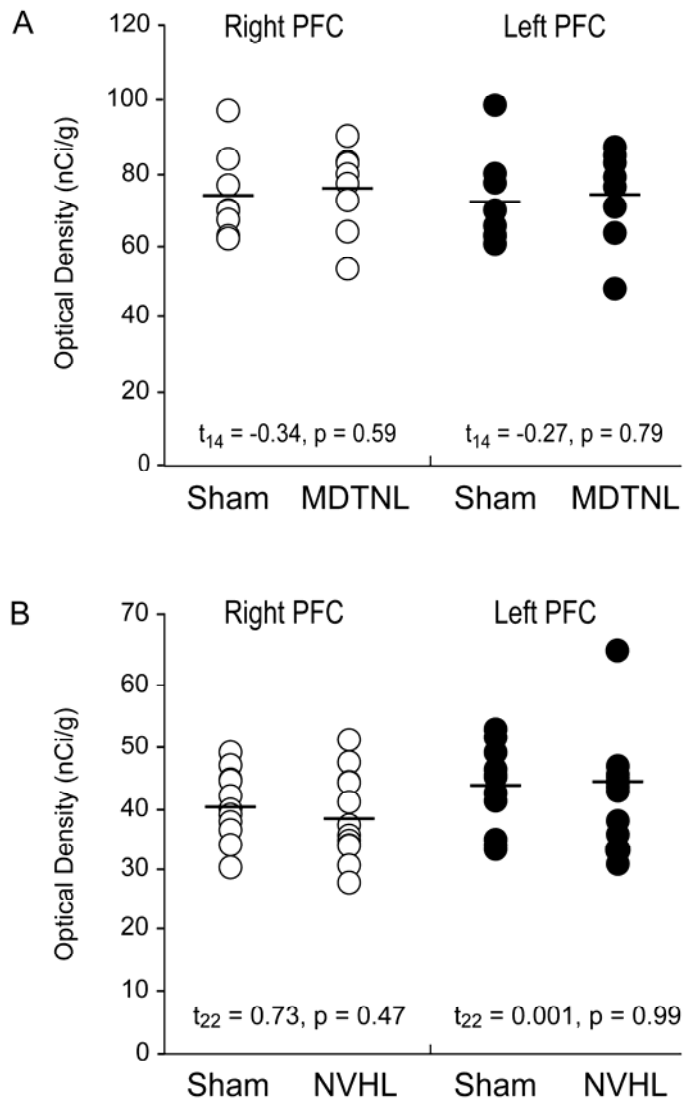
a The mean expression levels of δ mRNA were significantly reduced in layers 3 (16%), 4 (18%), 5 (23%) and 6 (18%) in subjects with schizophrenia (closed bars) compared to control subjects (open bars). * $p < 0.01$, ** $p < 0.0001$

Figure S4. Expression levels of NMDA Nr1 (A-C) and GABA_A δ (D-F) mRNAs in the frontal cortex of a wild type mouse (A,D), a mouse heterozygous for the Nr1 neo locus (Nr1^{neo/+}; B,E) and a mouse homozygous for the Nr1 neo locus (Nr1^{neo/neo}; C, F)^a



^a The densities of hybridization signals are presented in a pseudocolor manner according to the calibration scales (right) for each transcript. Note the progressive decrease in mRNA expression of NMDA Nr1 subunit as a function of genotype. In contrast, the mRNA levels of δ subunit do not appear to differ across genotypes (D-F). MFC is represented in the autoradiograms as the area between the solid lines. Scale bar = 500 μm. Consistent with these qualitative observations, mean NMDA Nr1 subunit mRNA levels (G) were significantly reduced by 45% in the MFC of Nr1^{neo/neo} mice compared to wild type mice, and the levels in the Nr1^{neo/+} mice were intermediate. In contrast, mean mRNA levels of δ subunit (H) did not differ as a function of genotype. Groups not sharing the same letter are statistically different at $p < 0.05$.

Figure S5. Expression levels δ subunit mRNA in MDTNL (A) and NVHL (B) rats^a



^a Neither adult lesions in the MDTN or neonatal lesions to the ventral hippocampus had an effect on the mRNA levels of δ subunit.

Table S1. Characteristics of human subjects used in this study

Control Subjects									Subjects with Schizophrenia									
Pair	Case	Sex/ Race	Age (years)	PMI ^a	Storage Time ^b	RIN	pH	Cause of Death ^c	Case	DSM IV Diagnosis	Sex/ Race	Age (years)	PMI ^a	Storage Time ^b	RIN	pH	Cause of Death ^c	Benzodiazepines/ Mood Stabilizers/ Antidepressants/ATO D
1	592	M/B	41	22.1	112.1	9.0	6.7	ASCVD	533	Chronic undifferentiated schizophrenia	M/W	40	29.1	122.0	8.4	6.8	Accidental asphyxiation	N/N/N
2	567	F/W	46	15.0	116.2	8.9	6.7	Mitral Valve prolapse	537	Schizoaffective disorder ^d	F/W	37	14.5	121.2	8.6	6.7	Suicide by hanging	N/N/N
3	516	M/B	20	14.0	123.7	8.4	6.9	Homicide by gun shot	547	Schizoaffective disorder	M/B	27	16.5	119.8	7.4	7.0	Heat Stroke	Y/Y/Y
4	630	M/W	65	21.2	106.3	9.0	7.0	ASCVD	566	Chronic undifferentiated schizophrenia ^e	M/W	63	18.3	116.6	8.0	6.8	ASCVD	Y/N/Y
5	604	M/W	39	19.3	109.8	8.6	7.1	Hypoplastic coronary artery	581	Chronic paranoid schizophrenia ^{f,g}	M/W	46	28.1	114.4	7.9	7.2	Accidental combined drug overdose	Y/Y/N
6	546	F/W	37	23.5	120.1	8.6	6.7	ASCVD	587	Chronic undifferentiated schizophrenia ^e	F/B	38	17.8	113.0	9.0	7.0	Myocardial hypertrophy	Y/N/N
7	551	M/W	61	16.4	118.9	8.3	6.6	Cardiac Tamponade	625	Chronic disorganized schizophrenia ^h	M/B	49	23.5	106.9	7.6	7.3	ASCVD	N/N/Y
8	685	M/W	56	14.5	99.2	8.1	6.6	Hypoplastic coronary artery	622	Chronic undifferentiated schizophrenia ^d	M/W	58	18.9	107.0	7.4	6.8	Right MCA infarction	N/N/N
9	681	M/W	51	11.6	99.8	8.9	7.1	Hypertrophic cardiomyopathy	640	Chronic paranoid schizophrenia	M/W	49	5.2	104.9	8.4	6.9	Pulmonary embolism	N/N/Y
10	806	M/W	57	24.0	78.3	7.8	6.9	Pulmonary thromboembolism	665	Chronic paranoid schizophrenia ^f	M/B	59	28.1	102.5	9.2	6.9	Intestinal hemorrhage	N/N/Y
11	822	M/B	28	25.3	75.7	8.5	7.0	ASCVD	787	Schizoaffective disorder ^j	M/B	27	19.2	82.0	8.4	6.7	Suicide by gun shot	N/N/N
12	727	M/B	19	7.0	92.8	9.2	7.2	Trauma	829	Schizoaffective disorder ^{d,f,j}	M/W	25	5.0	73.7	9.3	6.8	Suicide by drug overdose	Y/Y/N
13	871	M/W	28	16.5	65.1	8.5	7.1	Trauma	878	Disorganized schizophrenia ^f	M/W	33	10.8	64.2	8.9	6.7	Myocardial fibrosis	N/Y/Y
14	575	F/B	55	11.3	114.9	9.6	6.8	ASCVD	517	Disorganized schizophrenia ^f	F/W	48	3.7	123.6	9.3	6.7	Intracerebral hemorrhage	N/N/N
15	700	M/W	42	26.1	96.9	8.7	7.0	ASCVD	539	Schizoaffective disorder ^k	M/W	50	40.5	121.0	8.1	7.1	Suicide by combined drug overdose	N/Y/Y
16	988	M/W	82	22.5	43.7	8.4	6.2	Trauma	621	Chronic undifferentiated schizophrenia ^d	M/W	83	16.0	107.3	8.7	7.3	Accidental asphyxiation	N/N/N
17	686	F/W	52	22.6	98.9	8.5	7.0	ASCVD	656	Schizoaffective disorder ^f	F/B	47	20.1	103.2	9.2	7.3	Suicide by gun shot	N/N/N
18	634	M/W	52	16.2	105.7	8.5	7.0	ASCVD	722	Chronic undifferentiated schizophrenia ^{i,l}	M/B	45	9.1	93.2	9.2	6.7	Upper GI bleeding	N/N/N
19	852	M/W	54	8.0	68.1	9.1	6.8	Cardiac tamponade	781	Schizoaffective disorder ^k	M/B	52	8	83.1	7.7	6.7	Peritonitis	N/N/Y
20	987 ^m	F/W	65	21.5	43.7	9.1	6.8	ASCVD	802	Schizoaffective disorder ^{f,l}	F/W	63	29	79.0	9.2	6.4	Right ventricular dysplasia	N/Y/N
21	818	F/W	67	24	76.9	8.4	7.1	Anaphylactic reaction	917	Chronic undifferentiated schizophrenia	F/W	71	23.8	56.9	7.0	6.8	ASCVD	N/N/N
22	857	M/W	48	16.6	67.0	8.9	6.7	ASCVD	930	Disorganized schizophrenia ^{i,k}	M/W	47	15.3	53.5	8.2	6.2	ASCVD	N/Y/N
23	739	M/W	40	15.8	91.9	8.4	6.9	ASCVD	933	Disorganized schizophrenia	M/W	44	8.3	52.9	8.1	5.9	Myocarditis	N/Y/Y
	Mean		48.0	18.0	92.4	8.7	6.9					47.9	17.8	96.6	8.4	6.8		
	SD		15.5	5.5	23.5	0.4	0.2					14.1	9.3	23.6	0.7	0.3		

^a PMI, postmortem interval in hours; ^b Storage time (months) at -80 C; ^c ASCVD, arteriosclerotic cardiovascular disease; ^d Subjects off medications at the time of death; ^e Alcohol abuse, in remission at the time of death; ^f Alcohol dependence, current at time of death; ^g Other substance abuse, current at time of death; ^h Alcohol abuse, current at time of death; ⁱ Other substance dependence, current at time of death; ^j Other

substance abuse, in remission at time of death;^k Alcohol dependence, in remission at time of death;^l Other substance dependence, in remission at time of death;^m History of post-traumatic stress disorder, in remission 39 years at time of death

Table S2. Macaque monkeys used in the developmental study

Age Groups	Animals	Age (months)	Perfusion Status	Prior Biopsy Status	Menstrual Phase
1W	RH193	.2	-	-	NA
	RH194	.2	-	-	NA
	RH199	.2	-	-	NA
	RH201	.2	-	-	NA
4W	RH197	1	-	-	NA
	RH200	1	-	-	NA
	RH209	1	-	-	NA
12W	RH192	3	-	-	NA
	RH198	3	-	-	NA
	RH203	3	-	-	NA
	RH212	3	-	-	NA
	RH230	3	+	-	NA
	RH234	3	+	-	NA
	RH241	3	+	-	NA
	RH245	3	+	-	NA
108W	RH261	9	-	-	NA
	RH262	9	-	-	NA
Pre-Puberty	RH240	16	+	-	NA
	RH255	17	+	-	NA
	RH264	15	+	-	NA
	RH265	15	+	-	NA
Post-Puberty	RH236	43	+	+	luteal
	RH238	44	+	+	follicular
	RH239	43	+	-	luteal
	RH246	43	+	+	follicular
	RH249	44	+	-	follicular
	RH258	47	+	-	follicular
Adult	RH248	93	+	+	luteal
	RH259	104	+	-	luteal
	RH260	138	-	-	luteal